International Journal of Antimicrobial Agents 67 (2026) 107946

Contents lists available at ScienceDirect

International Journal of Antimicrobial Agents

journal homepage: www.elsevier.com/locate/ijantimicag

An exploratory pharmacokinetic-pharmacodynamic analysis of ceftazidime-avibactam and various blood biomarkers in patients with hospital-acquired pneumonia or ventilator-associated pneumonia caused by *Klebsiella pneumoniae*

Amaury O'Jeanson[a], Elisabet I. Nielsen[a], Zoe Athanassa[b], Aghavni Ginosyan[a], Konstantinos Ioannidis[c], Sofia Manioudaki[b], Irina Petsa[b], Helen Giamarellou[d], Iosif Bader[b], Nikoletta Skarmoutsou[e], Evgenia Mylona[e], Aikaterini Sakagianni[b], Irena Loryan[a], Ilias Karaiskos[d,#], Lena E. Friberg[a,#,*]

[a] *Department of Pharmacy, Uppsala University, Uppsala, Sweden*
[b] *Intensive Care Unit, Sismanogleio General Hospital, Marousi, Greece*
[c] *Clinical Pharmacist, Hygeia General Hospital, Athens, Greece*
[d] *1st Department of Internal Medicine & Infectious Diseases, Hygeia General Hospital, Athens, Greece*
[e] *Department of Biopathology, Sismanogleio General Hospital, Athens, Greece*

ARTICLE INFO

Article history:
Received 3 December 2025
Accepted 21 July 2026

Editor: Dr Y-W Lin

Keywords:
Ceftazidime-avibactam
Population pharmacokinetics
Immune response biomarkers
Pharmacodynamics
Critically ill patients

ABSTRACT

Purpose: To characterise the pharmacokinetics (PK) of ceftazidime-avibactam (CAZ-AVI) and explore the dynamics of a broad blood immune biomarker panel in critically ill patients with hospital-acquired (HAP) or ventilator-associated pneumonia (VAP) caused by *Klebsiella pneumoniae*.

Methods: Population PK (PopPK) models were developed for CAZ and AVI individually and jointly, evaluating covariate effects and correlations at interindividual (IIV) and residual unexplained variability (RUV) levels. Biomarker turnover dynamics in blood were modelled, and exposure-biomarker relationships were assessed.

Results: The dataset included 266 drug plasma concentration measurements and 48–87 observations per biomarker, collected from ten critically ill patients. CAZ and AVI PK were well-described by two-compartment models, with estimated creatinine clearance (eCrCL) as a key covariate on clearance. Joint modelling revealed significant correlations between the two drugs at both IIV and RUV levels, supporting coherent patient-specific simulations. Turnover dynamics were characterised for 32 biomarkers. The most pronounced biomarker changes over the course of treatment were decreases in IL6, CRP and AREG, and increases in DCBLD2, LAMP3 and TRIM21. A significant exposure-response relationship was identified between CAZ plasma concentrations and CRP turnover, with higher CAZ levels associated with inhibition of CRP production.

Conclusions: The joint PopPK model confirmed eCrCL as a key covariate for clearance. Changes in 32 immune response biomarkers were quantified, with CRP showing a clear exposure-response relationship. These findings provide a foundation for prioritising biomarkers for future studies to guide therapeutic strategies in critically ill patients with HAP or VAP.

© 2026 The Author(s). Published by Elsevier Ltd. This is an open access article under the CC BY license (http://creativecommons.org/licenses/by/4.0/)

* Corresponding author. Mailing address: Department of Pharmacy, Uppsala University, Uppsala, Sweden.
E-mail address: lena.friberg@uu.se (L.E. Friberg).
# These authors contributed equally to this work.

https://doi.org/10.1016/j.ijantimicag.2026.107946
0924-8579/© 2026 The Author(s). Published by Elsevier Ltd. This is an open access article under the CC BY license (http://creativecommons.org/licenses/by/4.0/)

Take-home message

A joint population PK model for ceftazidime-avibactam in critically ill patients with HAP/VAP captures key variability and correlations between the two drugs, allowing consistent prediction of both drug concentrations within the same patient. Changes in multiple immune biomarkers, including a clear exposure-response relationship between ceftazidime and CRP, provide a foundation for prioritising biomarkers to guide future therapeutic strategies.

1. Introduction

The combination of ceftazidime (CAZ) with avibactam (AVI) has restored the bactericidal activity of CAZ against certain resistant Gram-negative pathogens, including strains of β-lactamase-producing *Klebsiella pneumoniae*. CAZ-AVI is today used to treat severe infections such as hospital-acquired pneumonia (HAP) and ventilator-associated pneumonia (VAP), particularly in critically ill patients where other therapeutic options may be limited [1–3].

In critically ill patients, complex pathophysiology changes lead to high interindividual variability (IIV) in both pharmacokinetics (PK) and immune responses. Optimising CAZ-AVI therapy is therefore challenging. Altered organ function, fluid shifts, or concomitant medications can substantially affect drug exposure, highlighting the need to characterise CAZ and AVI PK profiles to support individualised dosing strategies. Beyond PK, measurable blood biomarkers may offer complementary information on the host response and infection dynamics, thereby enabling more adaptive, patient-tailored treatment approaches.

Several approaches are currently available to personalise antibiotic therapy. Patient-specific characteristics such as renal function, approximated by the estimated creatinine clearance (eCrCL), are routinely used for a priori dose selection. In addition, therapeutic drug monitoring (TDM) allows adjustments of drug dosing to achieve pharmacokinetic/pharmacodynamic (PK/PD) targets associated with efficacy and/or toxicity [4,5]. TDM information can be further leveraged by integrating model-informed precision dosing (MIPD) to refine dose adjustments using pharmacometric approaches [6]. MIPD allows for individualised dosing through population PK (PopPK) models and Bayesian forecasting. However, the rapid physiological changes in critically ill patients introduce significant PK variability, making effective dose individualisation difficult in clinical practice.

Beyond drug concentration measurements, immune-related blood biomarkers have been suggested to be of value in individualisation [7,8]. While treatment individualisation has traditionally relied on the identification of the bacterial pathogen responsible for the infection and its susceptibility profile, biomarkers offer the possibility to extend personalisation strategies further – for example, informing decisions on when to stop treatment or when more intense or additional treatment is needed [8]. While concentration measurements focus on achieving appropriate drug exposure, biomarkers can provide a more comprehensive understanding by evaluating the host's physiological response to the infection and response to the treatment over time.

Such biomarkers may reflect not only the host immune response but also pathogen load, inflammatory processes and treatment efficacy, making them valuable tools for refining treatment strategies, particularly in critically ill patients with severe infection like HAP/VAP, where progression to life-threatening sepsis is a concern, and the duration of treatment for a successful outcome is unclear. In clinical practice, markers such as C-reactive protein (CRP) and procalcitonin are already used to support infection management, reflecting disease severity. However, additional biomarkers of interest, yet to be identified, could offer deeper insights into treatment needs, response to treatment, or requirements for dose adjustments.

Recent advances in multiplex immunoassay technologies, using panels designed to cover a wide array of proteins involved in specific disease pathways or biological processes [9], provide an opportunity to uncover such biomarkers. These could be integrated into a biomarker-based strategy quantitatively linking drug exposure to immune response biomarker dynamics (and ultimately to pathogen behavior), paving the way for more individualised and effective treatment approaches.

The aim of this study was to (i) describe the PopPK of CAZ and AVI in critically ill patients with HAP/VAP infected by *K. pneumoniae*, and (ii) explore whether the dynamics of a broad panel of immune-related biomarkers can be quantitatively described and linked to treatment response and drug exposure using nonlinear mixed-effects modelling. This exploratory analysis was intended to assess the feasibility of integrating biomarker information into pharmacometric frameworks and to identify potential candidate biomarkers that reflect disease progression and treatment response and support future MIPD strategies.

2. Materials and methods

2.1. Subjects

Patients were recruited between 01/03/2023 and 31/03/2024 at Hygeia and Sismanogleio General Hospitals (Athens, Greece). Eligible participants were critically ill adults ($\geq$18 years old) with Acute Physiology and Chronic Health Evaluation II (APACHE II) score $>$10 and/or Sequential Organ Failure Assessment (SOFA) score $>$3, a strong clinical, laboratory or imaging suspicion of HAP or VAP due to *K. pneumoniae*, and a clinical indication for CAZ-AVI treatment lasting $\geq$7 days.

Exclusion criteria included eCrCL $<$6 mL/min (Cockcroft-Gault), need for renal replacement therapy or extracorporeal membrane oxygenation, pregnancy, BMI $>$45 kg/m^2, active co-viral infection (e.g., COVID-19, influenza), or pulmonary comorbidities to confound treatment response (e.g., lung cancer, tuberculosis, cystic fibrosis, fungal infection, recent embolism).

Demographic (sex, age, weight, height), infection details (pathogen, $MIC_{CAZ/AVI}$), CAZ-AVI dosing history and co-medications were recorded. Daily assessments included SOFA scores, renal function (creatinine, cystatin C, urea, albumin), complete blood counts, lactate, CRP, procalcitonin and body temperature. Creatinine-based estimates of renal function were derived from daily plasma creatinine measurements using the Cockcroft-Gault, MDRD and CKD-EPI equations.

2.2. Ethics

The study protocol was approved by the local ethics committees at Hygeia (651/10-11-2021) and Sismanogleio (11/11.05.2023) General Hospitals. Written informed consent was obtained from all participants or their legal representatives. The handling of samples and data was approved by Uppsala University and conducted under the number 2023-05104-01. The study adhered to Good Clinical and Laboratory Practice standards.

2.3. Drug administration

CAZ-AVI (Zavicefta®, Pfizer) was administered at 2000/500 mg q8h as a two-hour intravenous infusion, diluted in 100 mL of normal saline [1]. Dose adjustments based on renal function were

made at the discretion of the treating physician in line with standard clinical practice.

2.4. Sampling

Venous blood samples were collected for both PK and biomarker analyses. PK sampling followed an optimal design analysis based on published PopPK models for CAZ and AVI [10], and was intended to support robust estimation of key model parameters (see Supplementary material). Samples were collected during the first dose and every other day (e.g., Days 3, 5, 7) until the end of treatment (EoT) within three defined sampling windows: (i) 15 min to 1 hour after infusion start (ascending), (ii) 15 min to 1 hour after infusion end (descending) and (iii) 15–20 min before the next dose (trough). The exact sampling times were recorded. For biomarker analysis, daily blood samples were collected from one day prior to treatment initiation through to the end of therapy. All blood samples were collected in sterile tubes containing EDTA as an anticoagulant. The blood samples were centrifuged at 2000 g for 10 min, and the plasma supernatant was transferred into polypropylene tubes. Plasma samples were frozen at −80°C within 30 minutes of collection.

2.5. Bioanalytical methods

Total plasma concentrations of CAZ and AVI were simultaneously quantified using Acquity ultra-performance liquid chromatography (UPLC) coupled with Xevo TQ-S Micro triple quadrupole mass spectrometer (MS/MS) (Waters Corporation, Milford, MA, USA). The lower limits of quantification were 0.1 µg/mL for CAZ and 0.05 µg/mL for AVI. Plasma protein binding of CAZ and AVI was assessed using equilibrium dialysis. Both the UPLC and equilibrium dialysis methods have been previously described [11]. Biomarker profiling was performed using the Olink Target 96 'immune response' panel (Olink Proteomics AB, Uppsala, Sweden), which comprises proteins involved in inflammation, immune signalling and host response pathways. No *a priori* selection of individual biomarkers was performed; instead, an exploratory approach was used to evaluate the broad range of immune-related proteins provided by this assay. CRP, procalcitonin and lactate were monitored as part of routine clinical care.

2.6. Microbiology

Bacterial identification and routine susceptibility testing were performed in the clinical laboratories of each participating hospital according to their standard protocols. Antimicrobial susceptibilities were tested using the VITEK® 2 system (bioMérieux, Marcy-l'Étoile, France) and interpreted according to EUCAST clinical breakpoints (susceptible ≤8 mg/L; resistant >8 mg/L) [12]. Carbapenemase gene content was detected using the NG-Test CARBA 5 immunochromatographic assay (NG Biotech, Guipry, France).

2.7. PK and biomarker analysis

Population PK models for CAZ and AVI were first developed separately. One-, two- and three-compartment structures were evaluated, along with alternative residual unexplained variability (RUV) and IIV models. A joint model was then developed to capture correlations between the two compounds. Covariate effects were assessed using a stepwise procedure, testing multiple demographic, clinical and renal function variables across relevant PK parameters. Simulations using the final joint model were compared with predictions from published PopPK models by Li et al. [10], based on matched covariates. Full model structures, selection criteria, model diagnostics and visual comparison methodology are detailed in the Supplementary material.

Biomarker modelling was performed using a three-step approach: (i) empirical trend analysis, (ii) turnover model development for dynamic biomarkers and (iii) exposure-response modelling based on individual-predicted CAZ plasma concentrations. Model evaluation was based on goodness-of-fit (GoF), visual predictive checks (VPCs) and objective function values (OFV). Details on model equations, assumptions and parameter estimation are provided in the Supplementary material.

Table 1
Demographics and biological characteristics of patients included in the study

Variable	n	Mean (SD)	Median	Range
Sex (F/M)	3/7			
Age (year)		66.2 (13.8)	69.5	32.0–84.9
Weight (kg)		85.4 (16.5)	85.0	60.0–120
Height (cm)		174 (9.04)	175	162–190
Total SOFA score[1]		5.26 (1.63)	5.50	3.00–9.00
Albumin (g/dL)[1]		2.52 (0.29)	2.50	2.10–3.00
Lactate (mmol/L)[1]		1.02 (0.85)	0.90	0.50–3.60
C-Reactive Protein (mg/L)[1]		81.9 (65.8)	97.0	8.79–230
Procalcitonin (µg/L)[1]		0.43 (29.1)	0.40	0.02–93.1
Serum creatinine (mg/dL)[1]		0.88 (0.58)	0.90	0.40–2.30
$eCrCL_{CG}$ (mL/min)[1]		103 (47.9)	110	37.1–190
$eCrCL_{CKD\text{-}EPI}$ (mL/min)[1,2]		171 (63.2)	201	59.0–238
$eCrCL_{MDRD}$ (mL/min)[1,2]		186 (89.6)	181	56.9–321

eCrCL: Estimated creatinine clearance. CG: Cockcroft-Gault. SOFA: Sequential Organ Failure Assessment.
[1] At the start of treatment.
[2] Obtained by multiplying the estimated glomerular filtration rate (eGFR, mL/min/1.73m^2) by the individual's body surface area (m^2).

2.8. PK/PD target attainment

To assess PK/PD target attainment for patients treated with CAZ-AVI, joint PK/PD indices were defined according to EUCAST recommendations [13]. For CAZ, antibacterial activity was evaluated as the proportion of the dosing interval during which the unbound plasma concentration exceeded the MIC ($fT > MIC$). A target of 100% $fT > MIC_{CAZ/AVI}$ at 8 mg/L (the EUCAST breakpoint for CAZ-AVI) was used. For AVI, β-lactamase inhibition was evaluated using the proportion of time that the unbound concentration remained above a threshold concentration ($fT > C_T$), with a target of 100% $fT > C_T$ at 1 mg/L [13].

2.9. Software

PK and biomarker modelling were performed using the ADVAN13 solver and first-order conditional estimation algorithm with interaction (FOCEI) in NONMEM (version 7.5, ICON plc, Dublin, Ireland). Pirana (version 2.9.6, Certara, Radnor, Pennsylvania, USA) was used as a modelling benchwork, and Pearl-speaks-NONMEM (PsN, version 5.3.0) as run manager. Data management and model evaluation were performed in R (version 4.2.1). Optimal design analysis was performed in R using the *mrgsolve* and *PopED* packages [14,15].

3. Results

3.1. Demographic and clinical data

Ten adult patients with HAP or VAP were included. Demographic and biological characteristics are summarised in Table 1.

At inclusion, the median total SOFA score was 5.5 (range: 3–9), which decreased to 3 (range: 0–6) at the EoT. The median change in SOFA score over the course of treatment was −3 (range: −5 to

0), indicating clinical improvement in nine patients, while one patient showed no change.

The median treatment duration with CAZ-AVI was 8.67 days (range: 7.67–13.7 days). All patients achieved clinical cure, with microbiological eradication or presumed eradication. All *K. pneumoniae* isolates were fully susceptible to CAZ-AVI (median $MIC_{CAZ/AVI}$ 2 mg/L; range: 1–8 mg/L).

The final PK dataset included 266 total concentration measurements (133 per drug) across up to six dosing intervals (sampling occasions) per patient. Protein binding was assessed in 51 plasma samples – selected to ensure representation from all patients and sampling occasions – with high fractions unbound (fu) for both CAZ (median fu 1.07; range: 0.93–1.25) and AVI (median fu 0.95; range: 0.80–1.24); the corresponding coefficients of variations were 7.55% and 10.3%, respectively. fu values exceeding 1 were attributed to analytical variability inherent to the equilibrium dialysis and bioanalytical assay.

The biomarker dataset comprised 5925 observations across 95 biomarkers. Of these, 62 measurements per biomarker were obtained from the Olink panel (based on 74 blood samples, of which 12 did not pass quality control), while routine clinical monitoring contributed measurements for CRP (87), procalcitonin (48) and lactate (86).

3.2. Single-drug PK analysis

The PK of both CAZ and AVI was adequately described by two-compartment disposition models. For both drugs, IIV was significant for clearance (CL) and volume of distribution in the central compartment (V1), with correlations between the two random-effects (ηs). Inclusion of eCrCL (Cockcroft-Gault) as a covariate on CL – modelled as a linear relationship (Eq. (1)) – significantly improved model fit (ΔOFV = −23.4 for CAZ; −22.3 for AVI). This covariate effect reduced IIV in CL from 65.5% to 27.8% for CAZ and from 75.7% to 32.6% for AVI.

$$CLeCRCL = (1 + THETA(x) \times (eCrCL - eCrCL_{median})) \quad (1)$$

Both models had a proportional RUV structure. All parameters were estimated with adequate precision, with relative standard errors (RSEs) below 30% for fixed effects and below 50% for random effects. GoF plots supported the adequacy of the structural and residual error models, and prediction-corrected VPCs (pcVPCs) showed that the final models adequately described the observed data. Parameter estimates and pcVPCs are provided in the Supplementary material.

3.3. Joint PK analysis

In the joint PopPK model for CAZ and AVI, incorporating correlation between the RUV terms from both drugs – alongside the use of the L2 data item method – significantly improved model fit (ΔOFV = −183). IIV in CL and V1 was shared between the two compounds, with no scaling required for V1 and a 1.14-fold higher IIV in CL for AVI compared to CAZ. In contrast, sharing the eCrCL covariate effect between the two drugs worsened model fit (ΔOFV = +5.69). Parameter estimates for the final joint model are provided in Table 2, with associated GoF plots available in the Supplementary material. The model adequately described observed plasma concentrations for both CAZ and AVI (Figs. 1A and B).

Visual comparisons with the published PopPK models by Li et al. revealed notable differences. Following the first dose (Figs. 2A and C), median maximum concentration (C_{max}) values predicted by the current model were approximately 1.4–1.6 times higher: 78.5 mg/L vs 54.4 mg/L for CAZ and 18.6 mg/L vs 11.1 mg/L for AVI. Differences in minimum (or trough) concentration (C_{min}) were even more pronounced – around 3–5 fold higher in the current study: 31.3 mg/L vs 10.6 mg/L for CAZ and 5.72 mg/L vs 1.16 mg/L for AVI. At steady state (Figs. 2B and D), these discrepancies became more substantial. Median steady-state C_{max} values were nearly doubled those predicted by Li et al.: 127 mg/L vs 67.7 mg/L for CAZ and 25.0 mg/L vs 12.7 mg/L for AVI. Steady-state C_{min} values were also notably higher: 59.9 mg/L vs 12.9 mg/L for CAZ and 8.69 mg/L vs 1.30 mg/L for AVI.

3.4. Biomarker analysis

An overview of the biomarker screening and modelling processes is provided in Fig. 3. In the initial screening step, 63 biomarkers were excluded due to negligible changes over time (defined as $k < 0.001\ h^{-1}$). Turnover models were then applied to the remaining 32 biomarkers, revealing increasing trends for seven and decreasing trends for 25 during treatment. Parameter estimates for all 32 biomarkers are available in the Supplementary material.

Among the increasing biomarkers, the most pronounced dynamics were observed for DCBLD2, LAMP3 and TRIM21, with estimated K_{in} values of 0.146 NPX/h, 0.0234 NPX/h and 0.00859 NPX/h, respectively. Estimated half-lives within this group ranged from 2.11 h (ITGA11) to 10.43 h (TRIM21). For the decreasing trend group, IL6, CRP and AREG exhibited the steepest declines, with k_{out} values of 0.00820 h^{-1}, 0.00628 h^{-1} and 0.00414 h^{-1}, respectively. Estimated half-lives within this group ranged from 84.5 h (IL6) to 759 h (BTN3A2). Time-course profiles for the six biomarkers with the most pronounced dynamics are illustrated in Fig. 4.

Turnover dynamics for 12 biomarkers – AREG, CKAP4, CLEC4C, CLEC4D, CLEC4G, CRP, DFFA, EIF4G1, HSD11B1, IL6, KRT19 and TRIM21 – were successfully characterised, with parameter estimates achieving acceptable precision (RSEs < 50%). The remaining 20 biomarkers were excluded from further modelling due to high uncertainty in parameter estimates.

In the final step, an exposure-response relationship was identified between individually-predicted CAZ total plasma concentration and CRP turnover. Given that CAZ was essentially unbound in plasma (fu ≈ 1; see Section 3.1), total concentrations were considered representative of unbound exposure. This relationship was best described by a slope effect inhibiting CRP production. Parameter estimates from this model are reported in Table 3. No significant exposure-response relationships were identified for the remaining 11 biomarkers.

3.5. PK/PD analysis

The lowest observed unbound trough concentrations were 13.0 mg/L for CAZ and 1.75 mg/L for AVI. Accordingly, all patients achieved the predefined joint PK/PD target for CAZ-AVI, corresponding to 100% of the dosing interval with unbound CAZ concentrations above the MIC ($fT > MIC_{CAZ/AVI}$, 8 mg/L) and 100% of the interval with unbound AVI concentrations above the threshold concentration for β-lactamase inhibition ($fT > C_T$, 1 mg/L).

4. Discussion

This exploratory study in critically ill patients with HAP or VAP caused by *K. pneumonia* characterised the PK of CAZ-AVI and investigated the dynamics of host-response biomarkers, including a panel of 92 immune markers and the routinely monitored variables CRP, procalcitonin and lactate. The joint PopPK model adequately described the PK of both CAZ and AVI using two-compartment models, with renal function (eCrCL) identified as a key covariate influencing CL. Significant correlations between the two drugs were characterised at both the IIV and RUV levels.

Table 2
Parameter estimates, associated relative standard errors (%RSE) and 95% confidence interval [95CI] for the final joint population pharmacokinetic model for ceftazidime-avibactam.

Parameter	Ceftazidime	Avibactam
θ_1: TVCL (L/h)	3.28 (13.1) [2.68–4.39]	4.78 (13.4) [3.77–6.27]
θ_2: TVV1 (L)	7.84 (34.6) [4.58–14.5]	7.21 (18.7) [4.87–9.88]
θ_3: TVQ (L/h)	24.4 (22.6) [15.2–37.1]	26.9 (18.6) [14.2–34.0]
θ_4: TVV2 (L)	19.3 (21.0) [11.0–26.5]	18.6 (22.6) [10.8–27.2]
θ_5: Linear eCrCL on CL[1]	0.00803 (20.0) [0.00425–0.0105]	0.00861 (16.3) [0.00567–0.0111]
θ_6: Scaling IIVCL[2]	-	1.14 (20.4) [0.680–1.60]
θ_7: Scaling IIVV1	-	1 FIX
IIV on CL (%)	28.5 (20.5) [22.0–34.0]	
IIV on V1 (%)	113 (26.2) [76.9–163]	
ω_{CL}-ω_{V1} correlation (%)	38.8 (23.8)	
RUV (proportional) (%)	29.6 (22.6) [24.0–36.7]	33.7 (20.8) [27.6–40.9]
σ_{CAZ}-σ_{AVI} correlation (%)	84.6 (16.3)	

Interindividual variability (IIV) associated with the typical value (TV) parameters is expressed as a coefficient of variation (%), calculated according to: $\sqrt{e^{\omega^2}-1} \times 100\%$.
[1] Coded as: $CLeCRCL = (1 + THETA(5) \times (eCrCL - 115))$.
[2] Coded as: $AVICL = TVAVICL \times AVICLeCRCL \times EXP(ETACAZCL \times THETA(6))$.

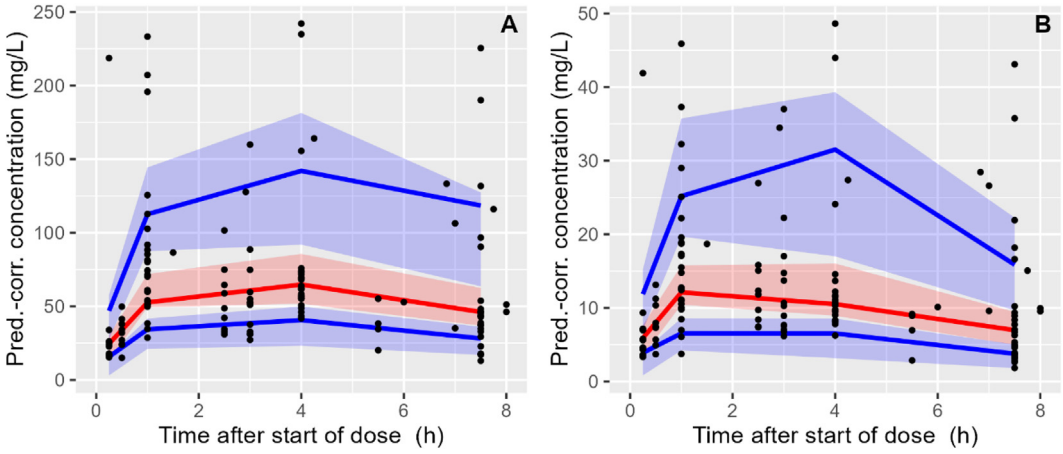

Fig. 1. Prediction-corrected visual predictive checks for the final joint population pharmacokinetic model for total plasma concentrations of ceftazidime (A) and avibactam (B). Solid red lines are the 50th percentiles of observations corrected by prediction, while solid blue lines represent the 5th and 95th percentiles. Shaded areas represent the 95% confidence intervals for the simulated 5th, median and 95th percentiles of the prediction-corrected observations.

Table 3
Parameter estimates, associated relative standard errors (RSE) and 95% confidence interval (95CI) for the exposure-response model between ceftazidime and CRP (slope effect inhibiting CRP production).

Parameter	Estimate	RSE (%)	95CI
θ_1: BASE (mg/L)	2.37 FIX	-	-
θ_2: KOUT (h^{-1})	0.00575	12.0	0.00464–0.00674
θ_3: DIFF (mg/L)	97.7	31.8	49.7–147
θ_4: SLOPE (h^{-1})	0.000299	19.9	0.000176–0.000385
IIV on DIFF (%)	140	20.6	86.1–255
RUV (proportional) (%)	33.3	7.63	29.0–38.6

Interindividual variability (IIV) associated with the typical value (TV) parameters is expressed as a coefficient of variation (%), calculated according to: $\sqrt{e^{\omega^2}-1} \times 100\%$.

Turnover dynamics could be characterised for 32 blood biomarkers, with DCBLD2, LAMP3 and TRIM21 showing the most pronounced increases during the study, and AREG, CRP and IL6 showing marked decreases. Turnover models for 12 immune biomarkers achieved acceptable precision (RSEs < 50%), and one significant exposure-response relationship was identified: higher CAZ plasma concentrations were associated with inhibition of the CRP production rate (K_{in}), resulting in reduced CRP turnover. The relationship was associated with high between-patient variability, in line with the observations. These findings indicate that while the PK of CAZ-AVI in this patient population was reasonably well described, the clinical relevance of biomarker-based exposure-response relationships warrants confirmation in larger studies.

The PK findings in this study align with those of Li et al. in key aspects. Both studies used two-compartment models to describe CAZ and AVI PK, and identified eCrCL as the major covariate influencing CL. This alignment reinforces the selection of Li et al.'s models as an appropriate basis for the optimal design analysis that informed our sampling approach. Interestingly, eCrCL calculated using the Cockcroft-Gault equation provided a better model fit (lower OFV) than MDRD or CKD-EPI estimates, despite the latter being generally preferred for critically ill populations. While Li et al. described more complex 'hockey-stick' relationships between CL and eCrCL, our study adopted a simpler linear relationship due to data limitations and the principle of parsimony. This approach still adequately captured the significant impact of eCrCL on drug clearance. However, the relatively sparse dataset (10 patients, 133 PK samples, 74 PD samples) likely limited the identification of additional covariates beyond eCrCL. Nonetheless, the consistent identification of renal function as a significant predictor of clearance reinforces its established clinical relevance for dose adaptation [1,10].

Median C_{max} and C_{min} values predicted by the joint model were notably higher than those predicted by Li et al.'s models for the same dosing regimen, particularly at steady-state. These differences likely reflect the lower typical CL values estimated in our study (3.28 vs 6.95 L/h for CAZ, and 4.78 vs 10.2 L/h for AVI). Importantly, these differences persisted even after adjust-

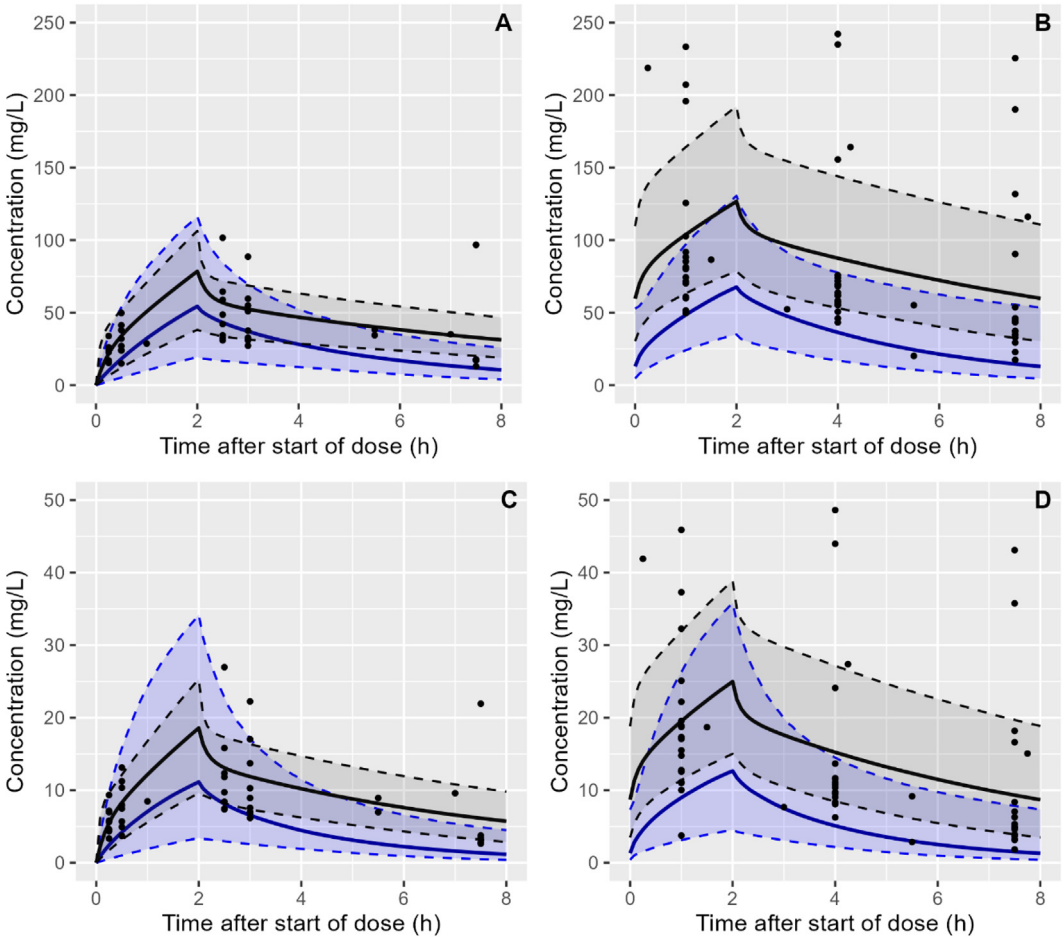

Fig. 2. Visual comparison plots for ceftazidime-avibactam at a dose of 2000/500 mg q8h (2h-infusion): (A) ceftazidime after first administration, (B) ceftazidime at steady-state, (C) avibactam after first administration and (D) avibactam at steady-state. Points represent observations from patients in the current study. Solid black lines and dashed black lines indicate 5th, median and 95th percentiles of the predictions from the final joint PopPK model. Solid blue lines and dashed blue lines indicate 5th, median and 95th percentiles of the predictions from the PopPK model by Li et al. [10].

ing the covariates in Li et al.'s models to reflect our study population, suggesting inherent differences in clearance and distribution characteristics between the two cohorts. Such differences may be driven by variations in disease severity, organ function, or other population-specific factors not captured by available covariates. The parameter estimates obtained from the joint model were very similar to those from separate single-drug models (Tables S1 and S2), i.e., the joint modelling approach did not introduce bias in the estimation of PK parameters. The observed differences between studies are more likely attributable to underlying population characteristics.

One individual in the current study exhibited markedly higher plasma concentrations than the rest of the cohort (Figs. 1 and 2). When this individual's data were excluded and the joint model re-estimated, IIV in CL decreased from 28.5% to 18.0% (32.5% to 25.7% for AVI after scaling adjustment), and IIV in V1 from 113% to 93.0%. Despite this reduction in variability, the resulting changes in median C_{max} and C_{min} values, after the first administration and at steady-state, were minimal (differences <7%). While the revised predictions moved slightly closer to those reported by Li et al., they remained consistently higher. This finding further supports the notion that differences between the two studies may arise from unaccounted population-specific factors.

The measured fu values for CAZ and AVI in this study were consistent with previous findings in patients undergoing continuous venovenous hemodiafiltration (CVVHDF) [11]. For CAZ, the median fu was 1.07 (range: 0.93–1.25), closely matching the values reported in CVVHDF patients (median: 1.07; range: 0.80–1.14), indicating negligible protein binding in both settings. In contrast, AVI had a higher median fu in the current study (median: 0.95; range: 0.80–1.24) compared to CVVHDF patients (median: 0.73; range: 0.55–0.92). Notably, the AVI fu observed here more closely matched the value reported in the SmPC (0.92) [1], suggesting a potential influence of renal replacement therapy on protein binding dynamics for AVI.

A key strength of this study was the identification of correlations between CAZ and AVI at both the IIV and RUV levels. This joint modelling approach maintained or improved model fit while ensuring robust estimation of fixed-effect parameters. The presence of shared IIV is mechanistically plausible, given the similar physicochemical and PK properties of CAZ and AVI. This suggests that variability in parameters such as CL or V1 for one drug is likely reflected in the other. By jointly modelling both drugs and incorporating shared variability and correlations, the model structure supports more coherent simulation of CAZ-AVI concentration-time profiles within the same individual. This enhances the model's utility for realistic, patient-specific simulations [16,17], which is particularly valuable for clinical applications such as TDM and model-informed precision dosing for β-lactam/β-lactamase inhibitor combinations. In practice, such a framework may reduce the need to monitor both drugs, as measurement of one compound could provide sufficient information to guide dos-

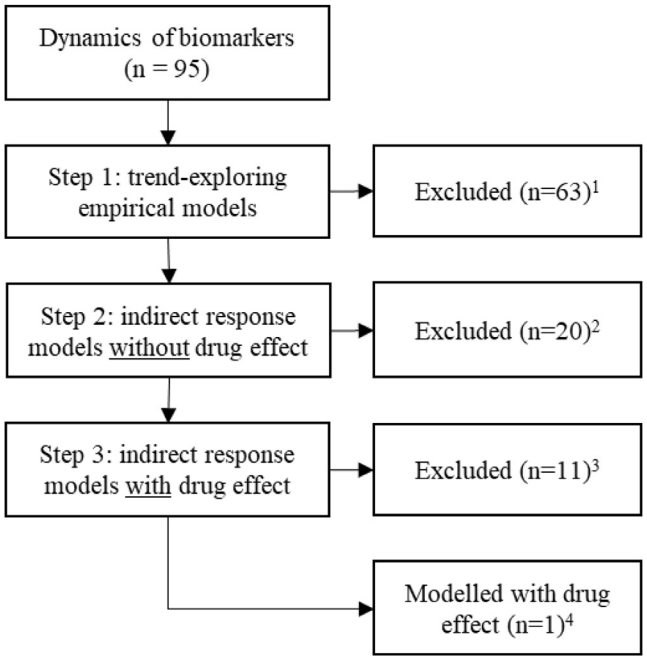

Fig. 3. Flow chart of the biomarker analysis.
[1]Excluded biomarkers due to flat trend ($k < 0.001\ h^{-1}$): BIRC2, CCL11, CD28, CD83, CDSN, CLEC4A, CLEC6A, CLEC7A, CNTNAPP2, CXADR, CXCL12, DAPP1, DDX58, DGKZ, DPP10, EDAR, EGLN1, FAM3B, FCRL3, FCRL6, FGF2, GALNT3, GLB1, HCLS1, HEXIM1, HNMT, ICA1, IFNLR1, IL2RB1, IL5, IRAK1, IRF9, ITGA6, ITGB6, ITM2A, JUN, KLRD1, Lactate, LAG3, LILRB4, LY75, MASP1, MGMT, MILR1, NF2, NFATC3, NTF4, PLXNA4, PPP1R9B, PRDX1, PRDX3, PRDX5, PRKCQ, Procalcitonin, PTH1R, SH2B3, SH2D1A, SPRY2, STC1, TANK, TPSAB1, TRAF2, TRIM5.
[2]Excluded biomarkers due to unreliable turnover estimates (RSE ≥ 50%): ARNT, BACH1, BTN3A2, DCBLD2, DCTN1, EIF5A, FXYD5, IL10, IRAK4, ITGA11, KPNA1, LAMP3, NCR1, PADI2, PIK3AP1, PSIP1, SIT1, SRPK2, TREM1, ZBTB16.
[3]Excluded biomarkers due to no significant drug effect (ΔOFV < 3.84): AREG, CKAP4, CLEC4C, CLEC4D, CLEC4G, DFFA, EIF4G1, HSD11B1, IL6, KRT19, TRIM21.
[4]Biomarker successfully modelled with a drug effect: CRP.

ing decisions, thereby aiding in the optimisation of dosing regimens [18].

For the biomarker analysis, although the dataset was rich and well-suited to track treatment-related changes, the lack of informative baseline measurements – particularly in the absence of disease – posed significant challenges. Because all patients were recruited at the point of requiring treatment, biomarker levels prior to infection or clinical deterioration could not be collected. This complicated the distinction between natural disease progression and potential drug-induced effects, especially since estimation of K_{in} and the biomarker baseline is interdependent with k_{out} (as $K_{in} = BASE \times k_{out}$ in a healthy state). In addition, the model structure assumed a single directional change from treatment initiation (i.e., increase or decrease from baseline), which may not fully capture more complex clinical biomarker profiles, such as delayed peaks or transient increases before resolution.

An additional limitation was that the Olink platform provides relative quantification (NPX, normalised protein expression) rather than absolute concentrations. While NPX values are internally consistent within an assay, they cannot be directly compared across cohorts or studies without bridging (i.e., common reference samples). This further obscured the definition of true baseline levels and prevented alignment with biomarker reference values reported in the literature. To address this, baseline values were fixed during modelling.

Despite these limitations, changes in biomarker dynamics during treatment were observed and could be characterised for 32 biomarkers, although the precision of parameter estimates varied. Among commonly used clinical infection biomarkers such as CRP, IL6, and procalcitonin, only CRP demonstrated a significant exposure-response relationship. IL6 dynamics could be adequately characterised using a turnover model, but did not show a significant exposure-response relationship, while the procalcitonin did not support robust model characterisation. Several biomarkers (AREG, CRP, DCBLD2, IL6, LAMP3 and TRIM21) showed pronounced changes and may be promising candidates for describing disease resolution in future studies. In the case of CRP, although a statistically significant exposure–response relationship with CAZ concentrations was identified, the effect size was modest and associated with substantial interindividual variability. This likely reflects the indirect and multifactorial nature of CRP dynamics, which is influenced not only by antibiotic exposure but also by host immune response and infection progression. The relationship should be interpreted cautiously and needs further evaluation to support CRP as a biomarker being related to drug exposure.

For CRP, the estimated half-life was 110 hours, longer than the 4–62 hours half-lives reported in the literature [19–24]. IL6 exhibited a half-life of 84 hours, compared with ∼1 hour typically observed in critical care settings [25,26], but closer to values reported in breast cancer patients with febrile neutropenia (49 h) [24], patients undergoing bone marrow transplantation (21 h) [27], or orthopedic surgery (15 h) [28]. Such estimates represent apparent *in vivo* half-lives and may vary with biological context and the method used for their determination. The observed discrepancies likely reflect limitations of the modelling framework in the absence of true baseline measurements, as estimation of baseline, K_{in}, and k_{out} parameters is interdependent. Furthermore, the assumed turnover structure may lead to inflated apparent half-lives when biomarker dynamics include delayed inflammatory progression or transient increases following treatment initiation before subsequent decline. As a result, the derived half-lives should be interpreted as effective parameters describing the observed time course of biomarker changes under treatment, rather than as direct physiological turnover rates. For other biomarkers, turnover rates could not be compared due to the lack of published reference values in similar settings. Nonetheless, these trends provide valuable insights into the dynamics of host-response markers during antibiotic therapy.

The heterogeneity in biomarker dynamics likely reflects the complex and diverse nature of the host immune response to infection. The evaluated biomarkers represent various biological functions, including pro-inflammatory signalling, immune cell activity and regulatory processes, and are therefore not expected to show uniform profiles over time during treatment. This biological diversity, together with interindividual differences in disease severity and host response, likely contributes to the observed variability and limits the identification of consistent exposure–response relationships. A functional annotation of the evaluated biomarkers is provided in the Supplementary material.

CAZ plasma concentration-time profiles were used to drive the response in the turnover models, which described the dynamics of the biomarkers. MIC-normalised PK/PD indices (e.g., $fT > MIC$) are time-static measurements and would not capture the time-varying effects [29]. It should be noted that any time-varying activity of AVI was not accounted for.

Further studies in larger and more diverse patient populations are needed to better characterise the potential interplay between drug exposure and biomarker dynamics, and ultimately clinical outcomes. Including healthy volunteers could help establish disease-free baselines, enabling clearer differentiation between natural disease progression and drug-related effects. Extending post-treatment follow-up in patients may also support character-

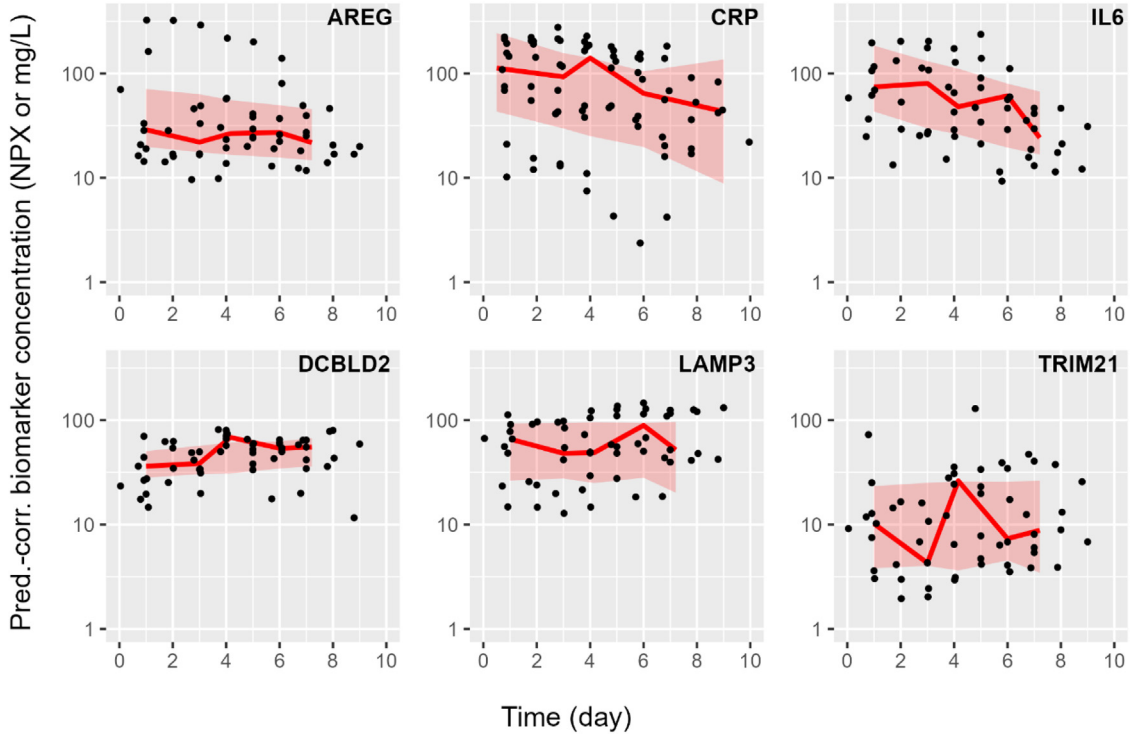

Fig. 4. Prediction-corrected visual predictive checks for biomarker turnover models without drug effects for biomarker plasma concentrations during treatment. Biomarkers exhibiting decreasing trends are shown in the upper row (AREG, CRP, IL6), while biomarkers exhibiting increasing trends are shown in the lower row (DCBLD2, LAMP3, TRIM21). Red solid lines indicate the median of the prediction-corrected observations, and shaded areas represent the 95% confidence intervals of the simulated median prediction-corrected observations. Prediction-corrected observations were grouped into time bins to calculate the observed and simulated medians. AREG: Amphiregulin (NPX); CRP: C-reactive protein (mg/L); IL6: Interleukin 6 (NPX); DCBLD2: Discoidin, CUB and LCCL domain containing 2 (NPX); LAMP3: Lysosomal associated membrane protein 3 (NPX); TRIM21: Tripartite motif containing 21 (NPX).

isation of biomarker return to baseline, providing insight into host recovery and longer-term treatment effects. While late-phase measurements may be informative, the early phase of treatment remains the most clinically relevant for guiding therapeutic decisions. Further research should focus on improving our understanding of early biomarker changes and their potential role in predicting treatment response and optimising therapeutic strategies.

5. Conclusion

A joint PopPK model for CAZ and AVI was developed in critically ill patients with HAP or VAP, identifying significant IIV in V1 and CL, with eCrCL as a key covariate for CL variability. Correlations between the two drugs at both IIV and RUV levels enhance the model's clinical utility by enabling coherent, patient-specific simulations. Turnover dynamics for 32 biomarkers were characterised, with one significant exposure-response relationship identified between CAZ total plasma concentrations and CRP turnover. Although dataset limitations and the complexity of immune responses in critically ill patients warrant caution when extrapolating these findings, the study represents an initial step towards prioritising biomarkers for future studies aimed at optimising therapeutic strategies.

Funding: This work was supported by the European Union [grant number 861323]; and the Swedish Research Council [grant number 2022-00657].

Ethical Approval: The study protocol was approved by the local ethics committees at Hygeia (registration number: 651/10-11-2021) and Sismanogleio (11/11.05.2023) General Hospitals. The handling of samples and data was approved by Uppsala University and conducted under the number 2023-05104-01. The study was conducted in accordance with good clinical practice guidelines. All patients (or their legal representatives) provided written informed consent.

Availability of data and material: The data and materials used in this study are available upon request.

Authors' contribution: AOJ: Conceptualisation, Methodology, Formal analysis, Writing – original draft preparation, review & editing. EIN: Conceptualisation, Funding acquisition, Methodology, Supervision, Writing – review & editing. ZA: Investigation. AG: Formal analysis, Methodology, Validation. KI: Investigation. SM: Investigation. IP: Investigation. HG: Investigation. IB: Investigation. NS: Formal analysis, Validation. EM: Formal analysis, Validation. AS: Investigation. IL: Formal analysis, Methodology, Validation, Writing – review & editing. IK: Conceptualisation, Investigation, Supervision, Writing – review & editing. LEF: Conceptualisation, Funding acquisition, Methodology, Supervision, Writing – review & editing. The final submitted version of manuscript was reviewed and approved by all authors.

Declaration of competing interests: HG has received speaker honoraria from Pfizer and MSD. IK has received speaker honoraria from Pfizer, Menarini and bioMérieux. All other authors declare no conflict of interest.

Acknowledgments: The authors would like to extend our gratitude to the patients and their families for their participation in this study. The authors acknowledge the ICU staff from Hygeia General Hospital and Sismanogleio General Hospital for their exceptional assistance and support. The authors thank the Affinity Proteomics

Unit at SciLifeLab in Stockholm for supporting with protein semi-quantification (Olink Target 96).

Supplementary materials

Supplementary material associated with this article can be found, in the online version, at doi:10.1016/j.ijantimicag.2026.107946.

References

[1] Pfizer Zavicefta 2g/0.5g (ceftazidime/avibactam) powder for solution for infusion. European Medicine Agency (EMA) Summary of Products Characteristics (SmPC); 2021 https://www.ema.europa.eu/en/documents/product-information/zavicefta-epar-product-information_en.pdf Accessed October 30, 2025.

[2] Tichy E, Torres A, Bassetti M, Kongnakorn T, Di Virgilio R, Irani P, et al. Cost-effectiveness comparison of Ceftazidime/Avibactam versus Meropenem in the empirical treatment of hospital-acquired pneumonia, including ventilator-associated pneumonia, in Italy. Clinical Therapeutics 2020;42:802–17. doi:10.1016/j.clinthera.2020.03.014.

[3] Plata-Menchaca EP, Ferrer R. Current treatment of nosocomial pneumonia and ventilator-associated pneumonia. Rev Esp Quimioter 2022;35:25–9. doi:10.37201/req/s03.06.2022.

[4] Cusumano JA, Klinker KP, Huttner A, Luther MK, Roberts JA, LaPlante KL. Towards precision medicine: therapeutic drug monitoring–guided dosing of vancomycin and β-lactam antibiotics to maximize effectiveness and minimize toxicity. Am J Health-Syst Pharm 2020;77:1104–12. doi:10.1093/ajhp/zxaa128.

[5] Abdul–Aziz MH, Brady K, Cotta MO, Roberts JA. Therapeutic drug monitoring of antibiotics: defining the Therapeutic range. Therapeut Drug Monitor 2022;44:19. doi:10.1097/FTD.0000000000000940.

[6] Wicha SG, Märtson AG, Nielsen EI, Koch BCP, Friberg LE, Alffenaar JW, et al. From therapeutic drug monitoring to model-informed precision dosing for antibiotics. Clin Pharmacol Therapeut 2021;109:928–41. doi:10.1002/cpt.2202.

[7] Martínez ML, Plata-Menchaca EP, Ruiz-Rodríguez JC, Ferrer R. An approach to antibiotic treatment in patients with sepsis. J Thorac Dis 2020;12:1007–21. doi:10.21037/jtd.2020.01.47.

[8] Aulin LBS, Lange DW de, Saleh MAA, van der Graaf PH, Völler S, van Hasselt JGC. Biomarker-guided individualization of antibiotic therapy. Clin Pharmacol Therapeut. https://doi.org/10.1002/cpt.2194.

[9] Assarsson E, Lundberg M, Holmquist G, Björkesten J, Thorsen SB, Ekman D, et al. Homogenous 96-plex PEA immunoassay exhibiting high sensitivity, specificity, and excellent scalability. PLoS One 2014;9:e95192. doi:10.1371/journal.pone.0095192.

[10] Li J, Lovern M, Green ML, Chiu J, Zhou D, Comisar C, et al. Ceftazidime-Avibactam population pharmacokinetic modeling and pharmacodynamic target attainment across adult indications and patient subgroups. Clin Transl Sci 2019;12:151–63. doi:10.1111/cts.12585.

[11] O'Jeanson A, Ioannidis K, Nielsen EI, Galani L, Ginosyan A, Paskalis H, et al. Ceftazidime-avibactam (CAZ-AVI) pharmacokinetics in critically ill patients undergoing continuous venovenous hemodiafiltration (CVVHDF). Int J Antimicrob Agents 2025;65:107394. doi:10.1016/j.ijantimicag.2024.107394.

[12] European Committee on Antimicrobial Susceptibility Testing (EUCAST). Breakpoint tables for interpretation of MICs and zone diameters, version 15.0. 2025. https://www.eucast.org/fileadmin/src/media/PDFs/EUCAST_files/Breakpoint_tables/v_15.0_Breakpoint_Tables.pdf. Accessed October 30, 2025.

[13] European Committee on Antimicrobial Susceptibility Testing (EUCAST). Ceftazidime-avibactam: Rationale for the clinical breakpoints, version 1.0. 2020. https://www.eucast.org/fileadmin/src/media/PDFs/EUCAST_files/Rationale_documents/Ceftazidime-avibactam_Rationale_Document_20200730.pdf. Accessed October 30, 2025.

[14] Baron KT, Gastonguay MR. Simulation from ODE-based population PK/PD and systems pharmacology models in R with mrgsolve. J Pharmacokinet Pharmacodyn 2015;42:S84–5. doi:10.1007/s10928-015-9432-2.

[15] Nyberg J, Ueckert S, Strömberg EA, Hennig S, Karlsson MO, Hooker AC. PopED: an extended, parallelized, nonlinear mixed effects models optimal design tool. Comput Meth Prog Biomed 2012;108:789–805. doi:10.1016/j.cmpb.2012.05.005.

[16] Stein GE, Smith CL, Scharmen A, Kidd JM, Cooper C, Kuti J, et al. Pharmacokinetic and pharmacodynamic analysis of Ceftazidime/Avibactam in critically ill patients. Surg Infect 2018;20:55–61. doi:10.1089/sur.2018.141.

[17] Kidd JM, Stein GE, Nicolau DP, Kuti JL. Monte Carlo simulation methodologies for β-lactam/β-lactamase inhibitor combinations: effect on probability of target attainment assessments. J Clin Pharmacol 2020;60:172–80. doi:10.1002/jcph.1510.

[18] O'Jeanson A, Nielsen EI, Friberg LE. Therapeutic drug monitoring (TDM) of β-lactam/β-lactamase inhibitor (BL/BLI) drug combinations: insights from a pharmacometric simulation study. J Antimicrob Chemother 2025;80:79–86. doi:10.1093/jac/dkae375.

[19] Pepys MB, Hirschfield GM. C-reactive protein: a critical update. J Clin Invest 2003;111:1805–12. doi:10.1172/JCI200318921.

[20] Póvoa P, Coelho L, Dal-Pizzol F, Ferrer R, Huttner A, Conway Morris A, et al. How to use biomarkers of infection or sepsis at the bedside: guide to clinicians. Intensive Care Med 2023;49:142–53. doi:10.1007/s00134-022-06956-y.

[21] Clyne B, Olshaker JS. The C-reactive protein1. J Emerg Med 1999;17:1019–25. doi:10.1016/S0736-4679(99)00135-3.

[22] Vigushin DM, Pepys MB, Hawkins PN. Metabolic and scintigraphic studies of radioiodinated human C-reactive protein in health and disease. J Clin Invest 1993;91:1351–7. doi:10.1172/JCI116336.

[23] Takata S, Wada H, Tamura M, Koide T, Higaki M, Mikura SI, et al. Kinetics of c-reactive protein (CRP) and serum amyloid A protein (SAA) in patients with community-acquired pneumonia (CAP), as presented with biologic half-life times. Biomarkers 2011;16:530–5. doi:10.3109/1354750X.2011.607189.

[24] Netterberg I, Karlsson MO, Nielsen EI, Quartino AL, Lindman H, Friberg LE. The risk of febrile neutropenia in breast cancer patients following adjuvant chemotherapy is predicted by the time course of interleukin-6 and C-reactive protein by modelling. Br J Clin Pharmacol 2018;84:490–500. doi:10.1111/bcp.13477.

[25] Jawa RS, Anillo S, Huntoon K, Baumann H, Kulaylat M. Interleukin-6 in surgery, trauma, and critical care: part I: basic science. J Intensive Care Med 2011;26:3–12. doi:10.1177/0885066610395678.

[26] Jawa RS, Anillo S, Huntoon K, Baumann H, Kulaylat M. Interleukin-6 in surgery, trauma, and critical care part II: clinical implications. J Intensive Care Med 2011;26:73–87. doi:10.1177/0885066610384188.

[27] Machavaram KK, Almond LM, Rostami-Hodjegan A, Gardner I, Jamei M, Tay S, et al. A physiologically based pharmacokinetic modeling approach to predict disease–Drug interactions: suppression of CYP3A by IL-6. Clin Pharmacol Therapeut 2013;94:260–8. doi:10.1038/clpt.2013.79.

[28] Wirtz DC, Heller KD, Miltner O, Zilkens KW, Wolff JM. Interleukin-6: a potential inflammatory marker after total joint replacement. Int Orthop 2000;24:194–6. doi:10.1007/s002640000136.

[29] Friberg LE. Pivotal role of translation in anti-infective development. Clin Pharmacol Therapeut 2021;109:856–66. doi:10.1002/cpt.2182.